Pion structure explored in Minkowski space

Tobias Frederico
Instituto Tecnológico de Aeronáutica
São José dos Campos – Brazil
tobias@ita.br

Wayne de Paula (ITA)
Emanuel Ydrefors (ITA)
Jorge Alvarenga Nogueira (ITA/Roma I)
Giovanni Salmè (Roma)
Michele Viviani (Pisa)
Cedric Mezrag (Saclay)
Orlando Oliveira (Coimbra)
Bruno El-Bennich (Unicsul/SP)
João Pacheco B C de Melo (Unicsul/SP)
Vladimir Karmanov (Moscow)
Jaume Carbonell (IPN/Orsay)

Perceiving the Emergence of Hadron Mass through AMBER@CERN
6-7 August 2020 online

Outline

- Ingredients: quark-gluon vertex from LQCD data and gap equation
- quark-antiquark BSE for the pion (Minkowski space/LF wave function)
- Pion Electromagnetic form-factor, decay constant
- DA, PDF, TMD, GPD
- Summary

The Quark-Gap Equation and the Quark-Gluon Vertex

Spontaneous Chiral symmetry breaking & pion as a Goldstone boson
(origin of the nucleon mass – “constituent quarks”, Roberts, Maris, Tandy, Cloet, Maris...)

Schwinger-Dyson eq.
Quark propagator

Quark-gluon vertex

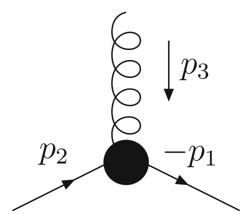

$$\Gamma^a_\mu(p_1, p_2, p_3) = g\, t^a\, \Gamma_\mu(p_1, p_2, p_3)$$

$$\Gamma_\mu(p_1, p_2, p_3) = \Gamma^{(L)}_\mu(p_1, p_2, p_3) + \Gamma^{(T)}_\mu(p_1, p_2, p_3)$$

Longitudinal component

$$\Gamma^{\mathrm{L}}_\mu(p_1, p_2, p_3) = -i\Big(\lambda_1\,\gamma_\mu \;+\; \lambda_2\,(\not p_1 - \not p_2)\,(p_1 - p_2)_\mu \;+\; \lambda_3\,(p_1 - p_2)_\mu \;+\; \lambda_4\,\sigma_{\mu\nu}\,(p_1 - p_2)^\nu\Big)$$

Rojas, de Melo, El-Bennich, Oliveira, Frederico, JHEP 1310 (2013) 193; Oliveira, Paula, Frederico, de Melo EPJC **78**(7), 553 (2018) & EPJC 79 (2019) 116 & Oliveira, Frederico, de Paula, EPJC 80 (2020) 484

INPUTS FROM LQCD in Landau gauge: SL momenta

Gluon propagator

$$D^{ab}_{\mu\nu}(q) = -i\,\delta^{ab}\left(g_{\mu\nu} - \frac{q_\mu q_\nu}{q^2}\right) D(q^2)$$

Dudal, Oliveira, Silva, Ann. Phys. **397**, 351 (2018)

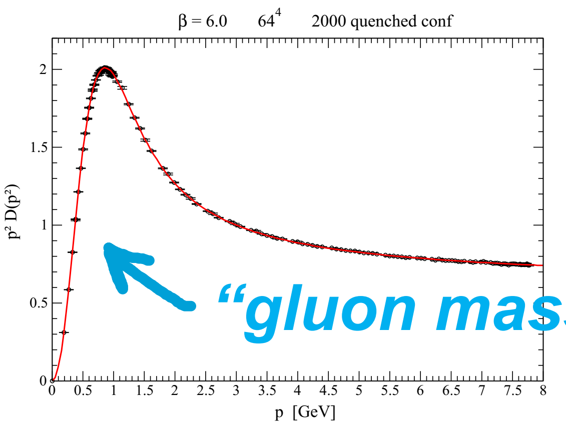

“gluon mass” ~ 500 MeV

Ghost propagator

$$D_{gh}(p^2) = \frac{F(p^2)}{p^2}$$

Duarte, Oliveira, Silva, PRD 94 (2016) 014502

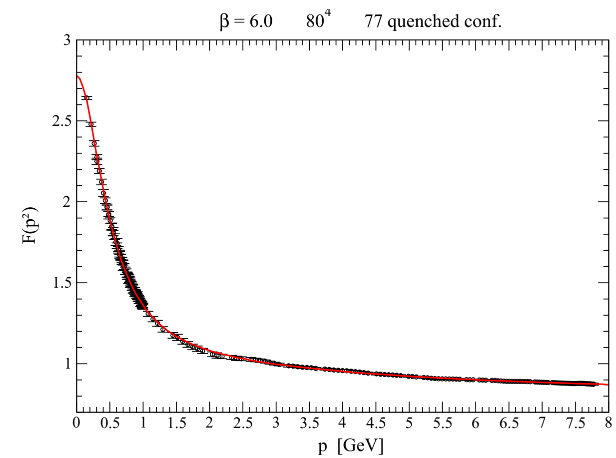

Quark propagator

Oliveira, Silva, Skullerud and Sternbeck, PRD 99 (2019) 094506

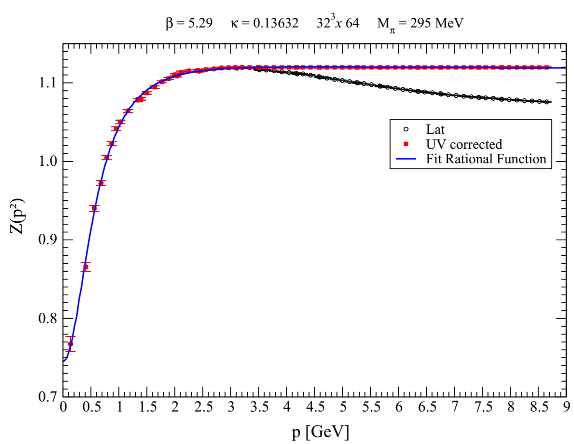

$$i\,Z(p^2)\,\frac{\not p + M(p^2)}{p^2 - M^2(p^2)}$$

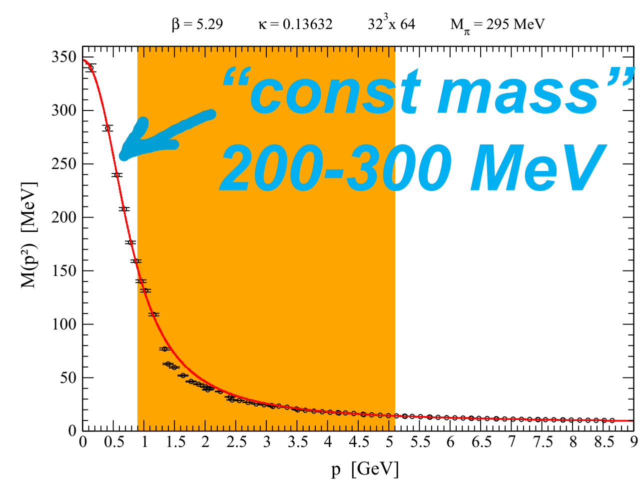

Parametrizations summarized in Oliveira, de Paula, Frederico, de Melo, EPJ C 79 (2019) 116

quark-gluon vertex from factors

- Slanov-Taylor identity & Quark-Ghost Kernel
- Padé approximants
- Error minimization ~ 2-4%
- simulating annealing

$\alpha_s = 0.22$ and all propagators renormalised at $\mu = 4.3\,\mathrm{GeV}$

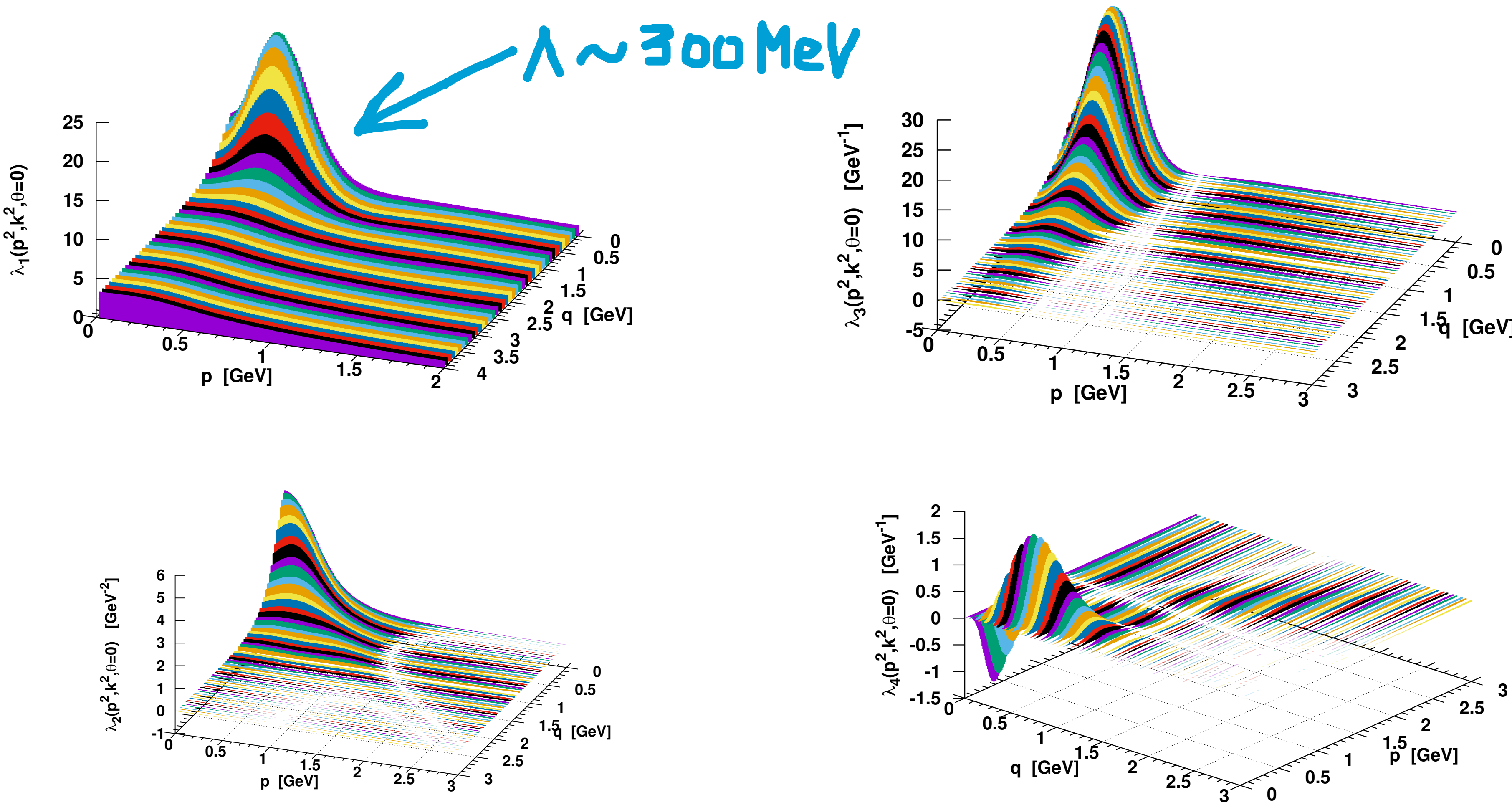

Oliveira, Frederico, de Paula, EPJC 80 (2020) 484

BSE quark-antiquark & pion model

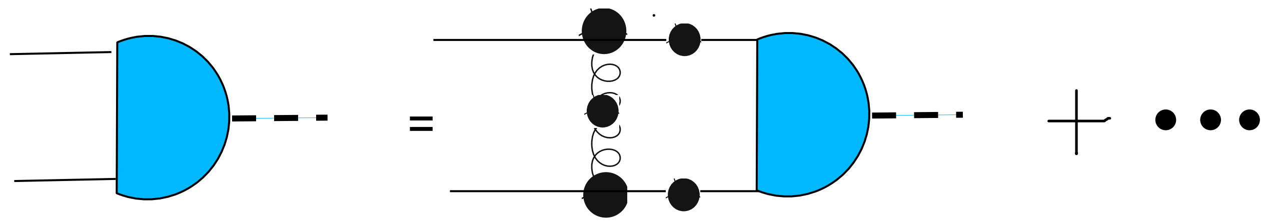

Ladder approximation (L): suppression of XL for Nc=3

[A. Nogueira, CR Ji, Ydrefors, TF, PLB777(2017) 207]

- constituent quark mass ~ 200 – 300 MeV
- Vector exchange

  Feynman gauge

  μ ~ 500 MeV

$$iK_V^{(Ld)\mu\nu}(k,k') = -ig^2 \frac{g^{\mu\nu}}{(k-k')^2 - \mu^2 + i\epsilon}$$

- quark-gluon vertex form-factor

  Λ ~ 300 MeV

$$\lambda_1 \gamma_\mu \qquad F(q) = \frac{\mu^2 - \Lambda^2}{q^2 - \Lambda^2 + i\epsilon}$$

SOLUTION IN MINKOWSKI SPACE

[pion mass → g]

Pion BS amplitude

$$\Phi(k,p) = S_1\phi_1 + S_2\phi_2 + S_3\phi_3 + S_4\phi_4$$

$$S_1 = \gamma_5 \quad S_2 = \frac{1}{M}\not{p}\gamma_5 \quad S_3 = \frac{k\cdot p}{M^3}\not{p}\gamma_5 - \frac{1}{M}\not{k}\gamma_5 \quad S_4 = \frac{i}{M^2}\sigma_{\mu\nu}p^\mu k^\nu\gamma_5$$

Main Tool: Nakanishi Integral Representation (NIR)

(Nakanishi 1962)

Each BS amplitude component:

$$\Phi(k,p) = \int_{-1}^{1} dz' \int_0^\infty d\gamma' \frac{g(\gamma',z')}{(\gamma' + \kappa^2 - k^2 - p.kz' - i\epsilon)^3}$$

$$\kappa^2 = m^2 - \frac{M^2}{4}$$

Bosons: Kusaka and Williams, PRD 51 (1995) 7026;

Light-front projection: integration in k⁻ Carbonell&Karmanov EPJA27(2006)1;EPJA27(2006)11;

TF, Salme, Viviani PRD89(2014) 016010,…

Fermions (0⁻): Carbonell and Karmanov EPJA 46 (2010) 387;

de Paula, TF,Salmè, Viviani PRD 94 (2016) 071901;

de Paula, TF, Pimentel, Salmè, Viviani, EPJC 77 (2017) 764

Generalized Stietjes transform and the LF valence wave function

Carbonell, TF, Karmanov PLB769 (2017) 418 (bosons)

$$\boxed{\Psi_i(\gamma,z;\kappa^2)=\int_0^{\infty} d\gamma' \frac{g_i(\gamma',z;\kappa^2)}{[\gamma+\gamma'+m^2z^2+(1-z^2)\kappa^2]^2}}$$

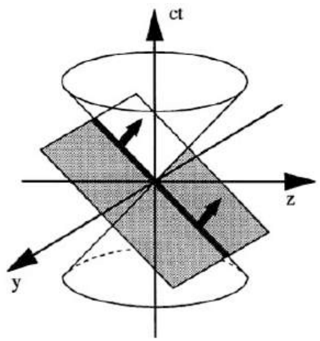

$$\gamma = k_\perp^2 \qquad z = 2x-1$$

BS amplittude

valence wf

$$\begin{tikzcd} \chi \arrow[rr, "\text{LF projection}"] & & \Psi_2 \arrow[dl, "\text{Inverse Stieltjes transform}"] \\ & g \arrow[ul, "\text{NIR}"] & \end{tikzcd}$$

J.H. Schwarz, J. Math. Phys. 46 (2005) 014501,

UNIQUENESS OF THE NAKANISHI REPRESENTATION

PHENOMENOLOGICAL APPLICATIONS from the valence wf → BSA!

Light-front amplitudes

B/m	M_π (MeV)	g^2	μ (MeV)	Λ/m	m (MeV)	p_{val}
1.35	140	26.718	430	1.0	215	0.68

Kernel has similar magnitude with LQCD form-factor ~ 50%

Ψ_1

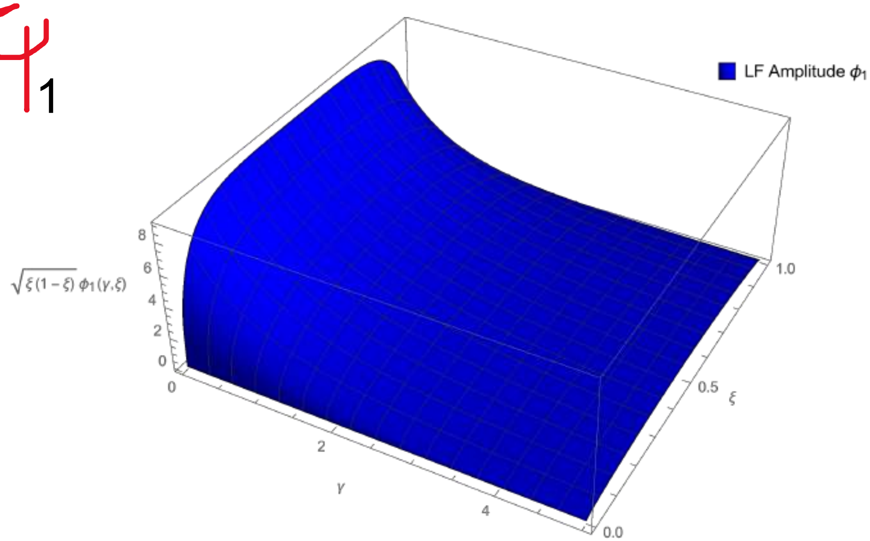

Ψ_2

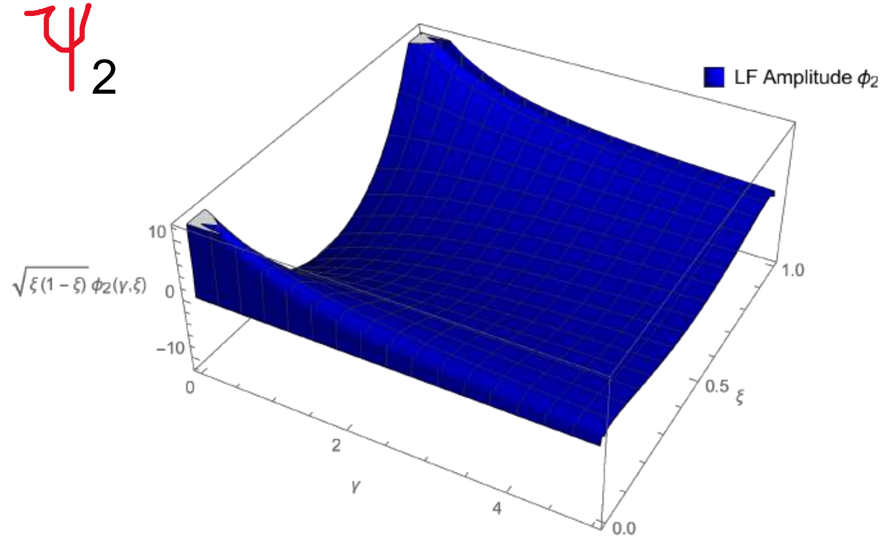

Ψ_3

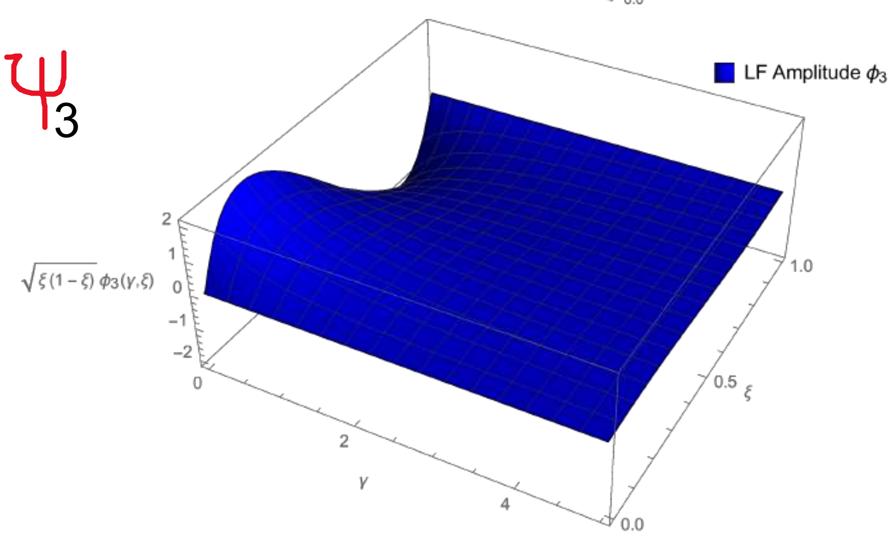

Ψ_4

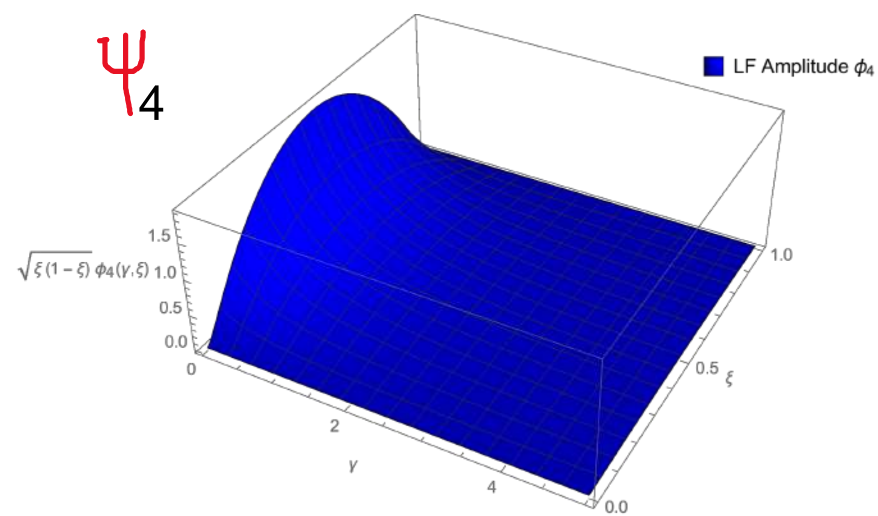

BS norm, valence wave function, decay constant

Normalization: $$i\, N_c \int \frac{d^4k}{(2\pi)^4} \left[\phi_1\phi_1 + \phi_2\phi_2 + b\phi_3\phi_3 + b\phi_4\phi_4 - 4\; b\phi_1\phi_4 - 4\frac{m}{M}\phi_2\phi_1\right] = -1$$

Valence wf:

$$\left\{\begin{aligned} \psi_{\uparrow\downarrow}(\gamma,z) &= -i\frac{M}{4p^+}\int\frac{dk^-}{2\pi}\mathrm{Tr}[\gamma^+\gamma_5\Phi(k;p)] \\ &= \psi_2(\gamma,z) + \frac{z}{2}\psi_3(\gamma,z) + \int_0^\infty \frac{d\gamma'}{M^3}\frac{\partial g_3(\gamma',z)/\partial z}{[\gamma+\gamma'+z^2m^2+(1-z^2)\kappa^2]} \\ \psi_{\uparrow\uparrow}(\gamma,z) &= \frac{\sqrt{\gamma}M}{4ip^+}\int\frac{dk^-}{2\pi}\mathrm{Tr}[\sigma^{+i}\gamma_5\Phi(k;p)] = \frac{\sqrt{\gamma}}{M}\psi_4(\gamma,z) \end{aligned}\right.$$

$$\gamma = k_\perp^2 \text{ and } z = 2\xi - 1$$

$$\Psi_i(\gamma,z;\kappa^2) = \int_0^\infty d\gamma'\frac{g_i(\gamma',z;\kappa^2)}{[\gamma+\gamma'+m^2z^2+(1-z^2)\kappa^2]^2}$$

Valence probability: $$P_{\rm val} = \frac{N_c}{16\,\pi^2}\int_{-1}^{1} dz \int_0^\infty d\gamma\ \left[|\psi^{\uparrow\downarrow}(\gamma,z)|^2 + |\psi^{\uparrow\downarrow}(\gamma,z)|^2\right]$$

Decay constant: $$f_\pi = -i\,\frac{N_c}{p^+}\int \frac{d^4k}{(2\pi)^4}\mathrm{Tr}[\,\gamma^+\,\gamma^5\,\Phi(p,k)] = \frac{2\,N_c}{M}\int \frac{d^2k_\perp}{(2\pi)^2}\frac{dk^+}{2\pi}\ \psi_{\uparrow\downarrow}(\gamma,z)$$

$$= -\frac{N_c}{2(2\pi)^2 M}\int_0^\infty d\gamma' \int_{-1}^{1} dz \int_0^\infty d\gamma \frac{g_2(\gamma,z)}{[\gamma+\gamma'+m^2z^2+(1-z^2)\kappa^2]^2}$$

increasing Pval

Set	m	B/m	μ/m	Λ/m	α_s ($\overline{\alpha}_s$)	P_{val}	$P_{\uparrow\downarrow}$	$P_{\uparrow\uparrow}$	f_π/m	f_π
I	187	1.25	0.15	2	5.146 (23.13)	0.64	0.55	0.09	0.414	77
II	255	1.45	1.5	1	52.78 (21.54)	0.65	0.55	0.10	0.433	112
III	215	1.35	2	1	76.28 (18.16)	0.67	0.57	0.11	0.453	98
IV	255	1.45	2	1	78.01 (18.57)	0.66	0.56	0.11	0.459	117
V	255	1.45	2.5	1	108.87 (16.87)	0.68	0.56	0.11	0.477	122
VI	255	1.45	2.5	1.1	87.66 (13.59)	0.69	0.56	0.12	0.498	127
VII	255	1.45	2.5	1.2	72.32 (11.21)	0.70	0.57	0.13	0.511	130
VIII	215	1.35	1	2	10.20 (8.50)	0.71	0.57	0.14	0.520	112
IX	187	1.25	1	2	9.96 (8.30)	0.71	0.58	0.14	0.514	96

TABLE I. Pion model with $m_\pi = 140$ MeV for different parameter sets, m and f_π in MeV. Calculated valence probability, total, antiparallel and parallel, and decay constant. The values of the coupling constant α_s and the effective strength, defined in Eq. (46), are also given.

$$\overline{\alpha}_s = \frac{\alpha_s}{\frac{\mu^2}{m^2}+0.2} \quad \text{with} \quad \alpha_s = \frac{g^2}{4\pi}(1-\mu^2/\Lambda^2)^2$$

Pion EM Form Factor

Alvarenga Nogueira, de Paula, TF, Mezrag, Ydrefors, Salmè in preparation

$$F(Q^2) = \frac{N_c}{2^5\pi^2 N_{Q_0}} \sum_{i,j=1}^{4} \int_0^\infty d\gamma \int_{-1}^{1} dz\, g_i(\gamma, z) \int_0^\infty d\gamma' \int_{-1}^{1} dz'\, g_j(\gamma', z') \int_0^1 dv\, v^2(1-v)^2\, c_{ij}$$

m	B/m	μ/m	Λ/m	f_π/m	P_{val}	f_π	r_π (fm)	r_{val} (fm)	r_{nval} (fm)
215	1.35	2	1	0.453	0.67	98	0.835	0.895	0.703
255	1.45	2.5	1.2	0.511	0.70	130	0.663	0.710	0.538

The experimental value of f_π is 130.50± 0.017 MeV

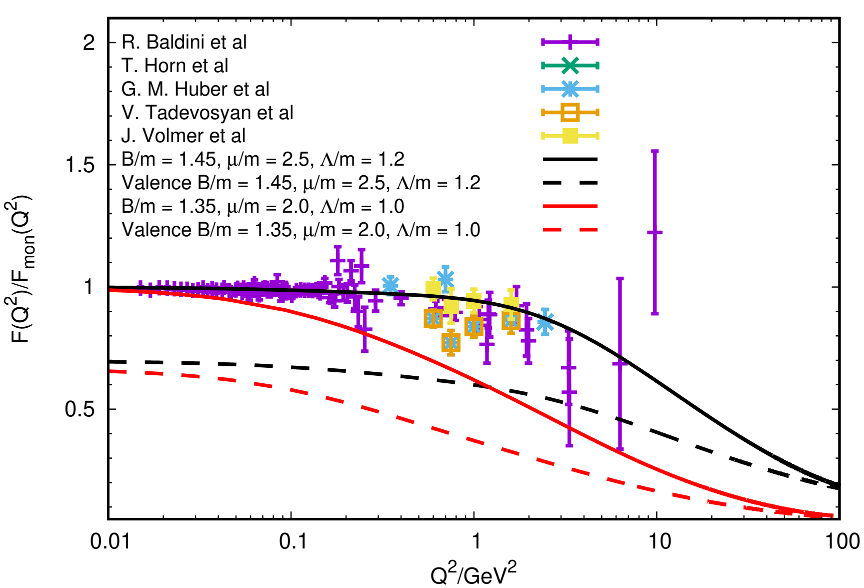

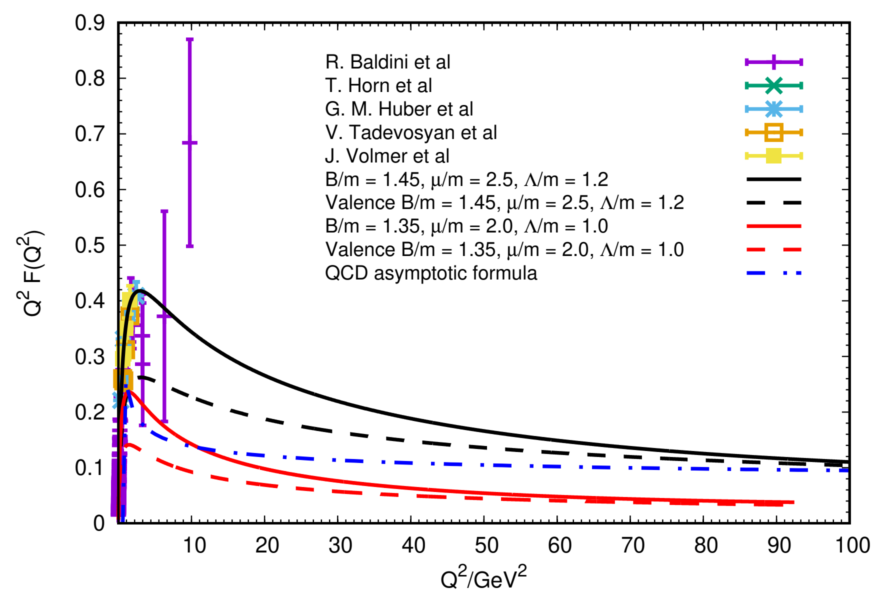

$$Q^2 F_{\mathrm{asymp}}(Q^2) = 8\pi\alpha_s(Q^2) f_\pi^2$$

G. Lepage, S. J. Brodsky, Phys. Lett. B 87 (1979) 359

Valence form factor

$$F_{\mathrm{val}}(Q^2) = \frac{N_c}{16\pi^3}\int d^2k_\perp \int_{-1}^{1} dz\Big[\psi^*_{\uparrow\downarrow}(\gamma', z)\psi_{\uparrow\downarrow}(\gamma'', z) + \frac{\vec{k}'_\perp \cdot \vec{k}''_\perp}{k'_\perp k''_\perp}\psi^*_{\uparrow\uparrow}(\gamma', z)\psi_{\uparrow\uparrow}(\gamma'', z)\Big]$$

$$\vec{k}'_\perp = \vec{k}_\perp + \frac{1}{4}(1-z)\vec{q}_\perp, \quad \vec{k}''_\perp = \vec{k}_\perp - \frac{1}{4}(1-z)\vec{q}_\perp = \vec{k'}_\perp - \frac{1}{2}(1-z)\vec{q}_\perp$$

Asymp. form factor $$F_{\mathrm{val}}(Q^2)|_{Q^2\to\infty} \sim \frac{N_c}{16\pi^2}\int_{-1}^{1} dz\, \psi_{\uparrow\downarrow}\left(\frac{(1-z)^2}{4}Q^2, z\right)\int_0^\infty d\gamma\, \psi_{\uparrow\downarrow}(\gamma, z)$$

$$F(Q^2) = \int_{-1}^{1} dz \tilde{F}(Q^2, z)$$

Valence pion GPD

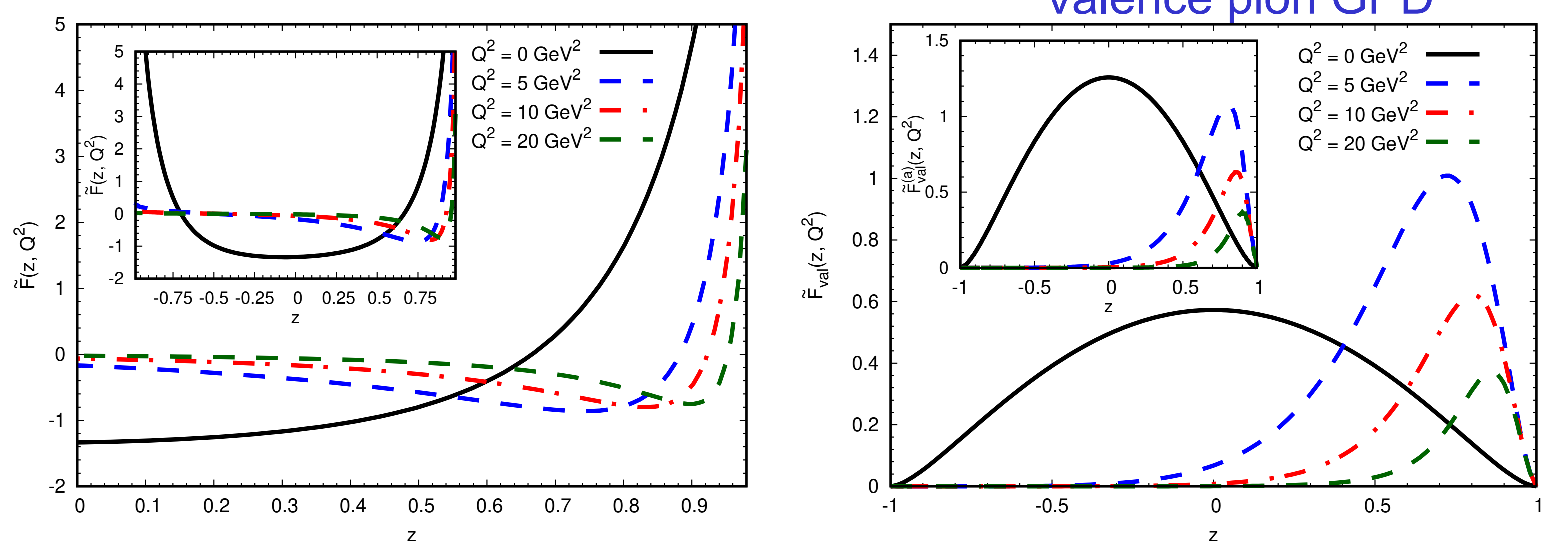

Figure 4: Left: Integrand of the full form factor vs z for fixed values of Q^2. In the main frame are shown the results for $z \geqslant 0$ and in the inset the results for the full interval are visible. Right: The corresponding results for the valence form factor. In the main frame the results obtained by using the complete formula are shown. In the inset the results for the asymptotic formula are displayed. For the visibility the results for $Q^2 > 0$ have been multiplied by a factor of 10.

$$F_\pi(Q^2) = \sum_n F_n(Q^2) = F_{val}(Q^2) + F_{nval}(Q^2)$$

$q\bar{q}$+gluons

$$r_\pi^2 = P_{val}\, r_{val}^2 + (1 - P_{val})\, r_{nval}^2$$

B = 1.45m_q m_{glue}= 2.5m_q Λ=1.2m_q m_q=255 MeV

r_π (fm)	r_{val} (fm)	r_{nval} (fm)
0.663	0.710	0.538

0.657 ± 0.003 fm   B. Ananthanarayan, I. Caprini, D. Das, Phys. Rev. Lett. 119 (2017) 132002

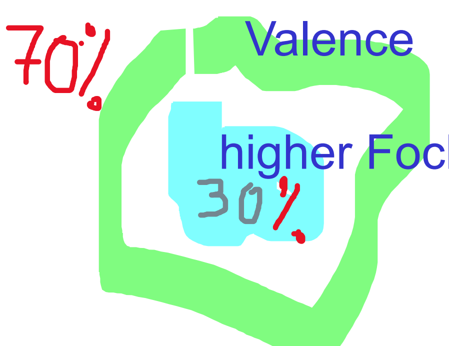

higher Fock-components → large virtuality→ more compact

Distribution and transverse amplitudes

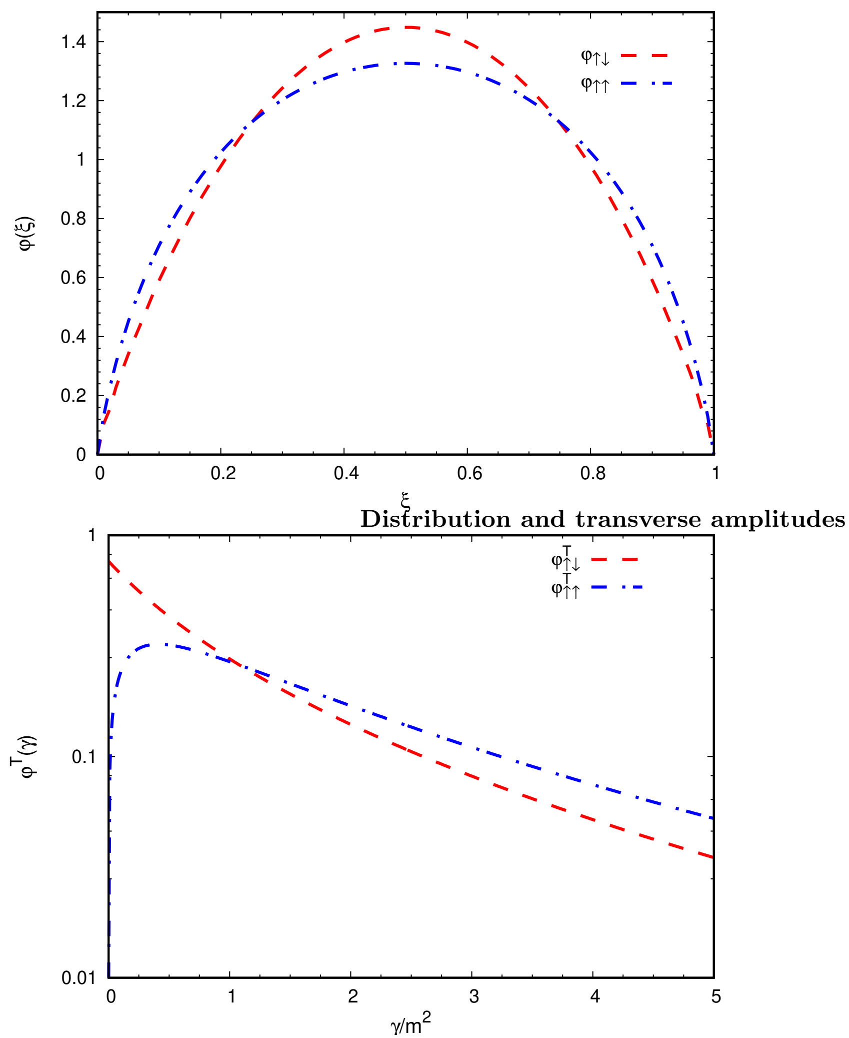

$$\varphi_{\uparrow\downarrow}(\xi) = \frac{\int_0^\infty d\gamma\, \psi_{\uparrow\downarrow}(\gamma, z)}{\int_0^1 d\xi \int_0^\infty d\gamma \psi_{\uparrow\downarrow}(\gamma, z)}\,,$$

$$\varphi_{\uparrow\uparrow}(\xi) = \frac{\int_0^\infty d\gamma \psi_{\uparrow\uparrow}(\gamma, z)}{\int_0^1 d\xi \int_0^\infty d\gamma \psi_{\uparrow\uparrow}(\gamma, z)}\,.$$

$$\varphi^T_{\uparrow\downarrow}(\gamma) = \frac{\int_0^1 d\xi\, \psi_{\uparrow\downarrow}(\gamma, z)}{\int_0^1 d\xi \int_0^\infty d\gamma\, \psi_{\uparrow\downarrow}(\gamma, z)}\,,$$

$$\varphi^T_{\uparrow\uparrow}(\gamma) = \frac{\int_0^1 d\xi\, \psi_{\uparrow\uparrow}(\gamma, z)}{\int_0^1 d\xi \int_0^\infty d\gamma\, \psi_{\uparrow\uparrow}(\gamma, z)}\,,$$

FIG. 4. Pion DA and transverse amplitudes for the two spin components obtained with the parameter set VII.

Valence TMD

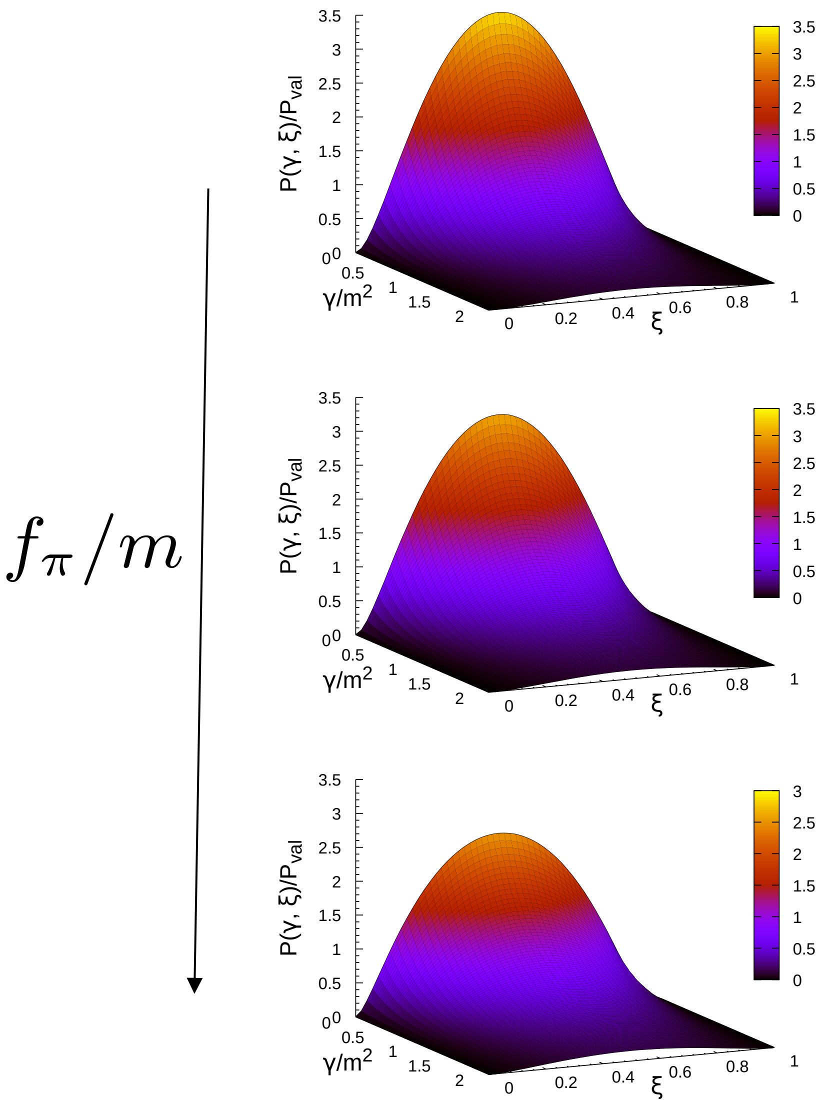

$$P_{\rm val} = \int_{-1}^{1} dz \int_{0}^{\infty} d\gamma \, \mathcal{P}_{val}(\gamma, z)$$

Set	f_π/m	$\eta_{\uparrow\downarrow}$	$\eta_{\uparrow\uparrow}$	η
II	0.433	1.71	1.50	1.66
IV	0.477	1.61	1.42	1.57
VII	0.511	1.44	1.26	1.40

TABLE II. Exponent of the fit function $(1-\xi)^\eta$ $(\xi \to 1)$ for the antiparallel, parallel and total valence distributions.

FIG. 3. 3D-valence momentum distribution as a function of ξ and $\gamma = k_\perp^2$. Panels from top to bottom represent the results for the parameter sets (II), (IV) and (VII), respectively.

Pion parton distribution $\xi\phi(\xi)$ at $Q^2 = 27\ \mathrm{GeV}^2$

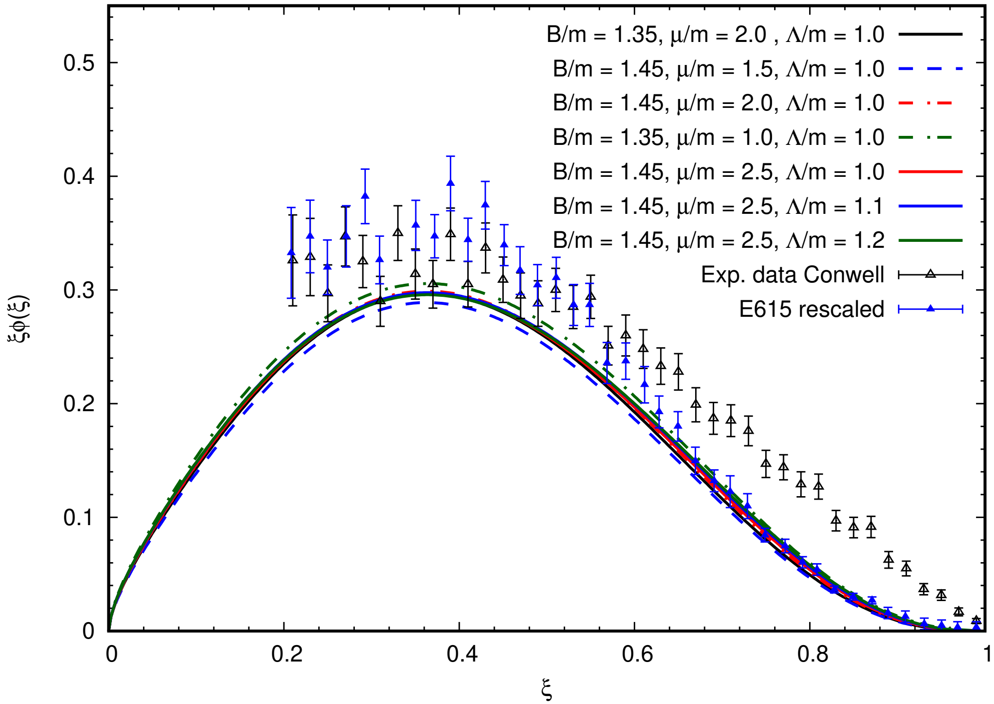

E615: Conway et al. PRD39 (1989) 92

E615 rescaled: Aicher, Schäfer, Volgesang PRL105 (2010) 252003

Middle panel: NLO evolved results for some of the parameters sets for $Q_0^2 = 0.25\ \mathrm{GeV}^2$ and $\alpha(Q_0^2) = 1.884$. Bottom panel: NLO evolution with the initial distribution $\xi\tilde{\phi}(\xi)$ from Eq. (49) for $\alpha(Q_0^2) = 1.884$.

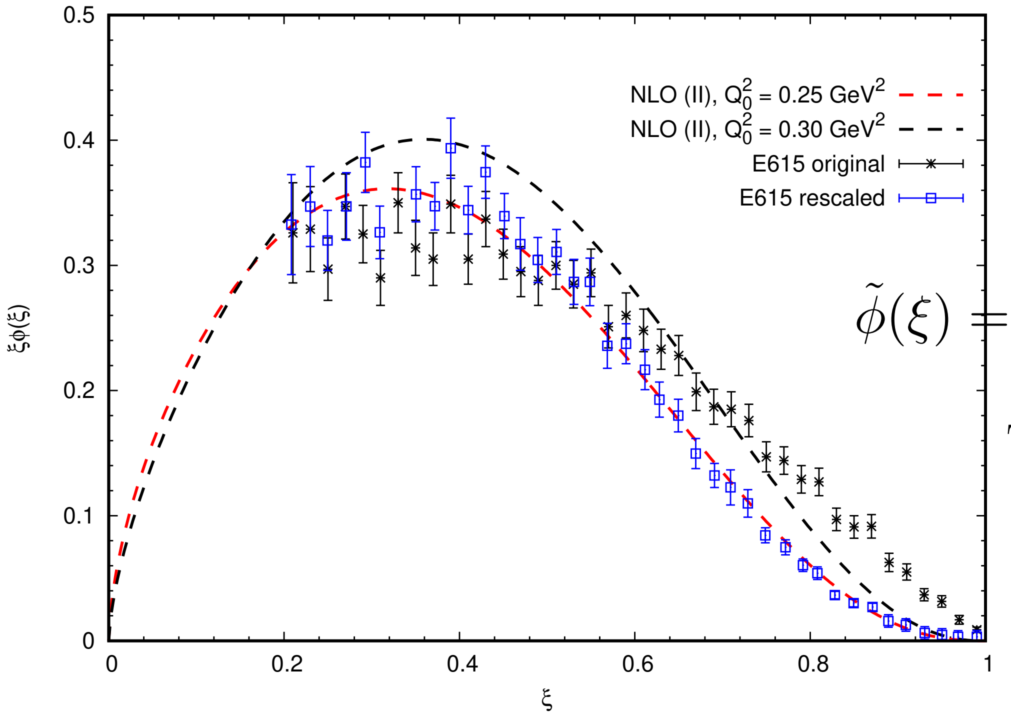

$$\tilde{\phi}(\xi) = \phi(\xi) + (1 - P_{val}) \int_\xi^1 \frac{dy}{y} \frac{\phi(\xi/y)}{P_{val}}$$

T. Frederico and G. Miller, Phys. Rev. D **50**, 210 (1994)

3D image of the pion on the null-plane

$$\{\xi = k^+/p^+, \mathbf{k}_\perp\} \xrightarrow{\text{F.T.}} \{\tilde{z} = p^+x^-/2, \mathbf{b}\}$$

Ioffe-time

Phys. Lett. B **30**, 123 (1969).

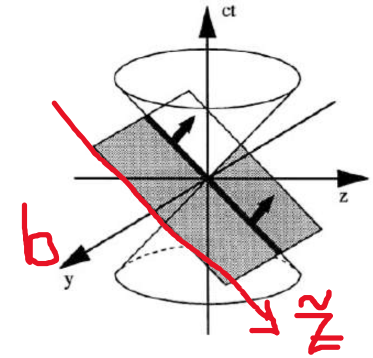

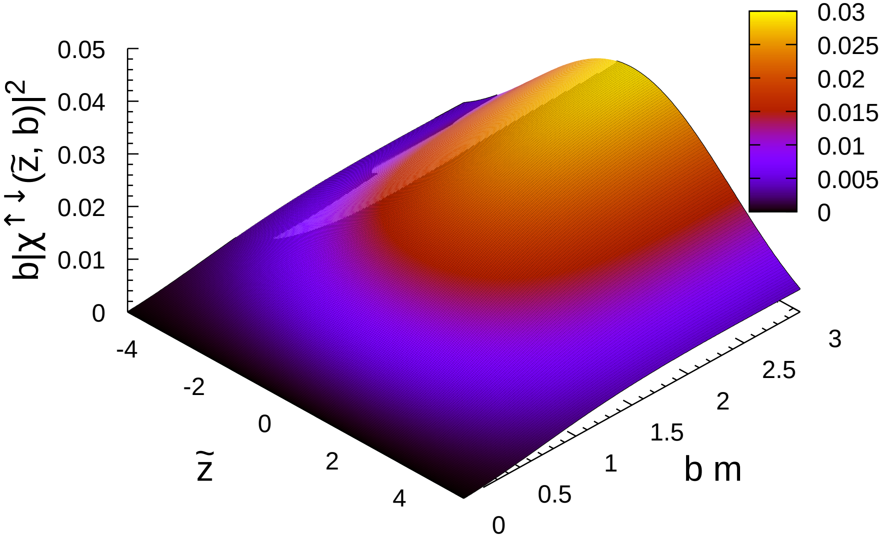

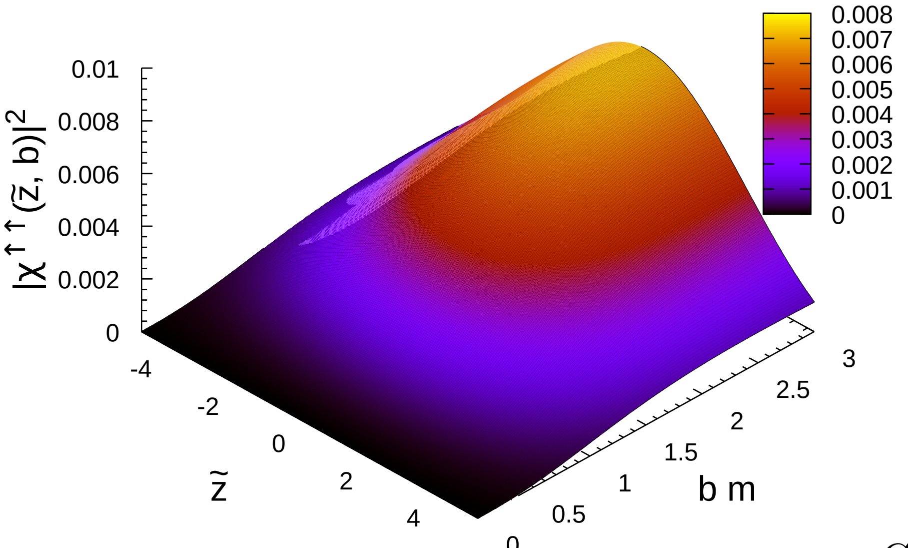

$$\tilde{\psi}_{\uparrow\downarrow}(\tilde{z}, b) = \mathrm{e}^{-b\,\kappa}\mathrm{e}^{-\frac{i}{2}\,\tilde{z}}\chi_{\uparrow\downarrow}(\tilde{z}, b)$$
$$\tilde{\psi}_{\uparrow\uparrow}(\tilde{z}, b) = \mathrm{e}^{-b\,\kappa}\mathrm{e}^{-\frac{i}{2}\,\tilde{z}}\chi_{\uparrow\uparrow}(\tilde{z}, b)$$

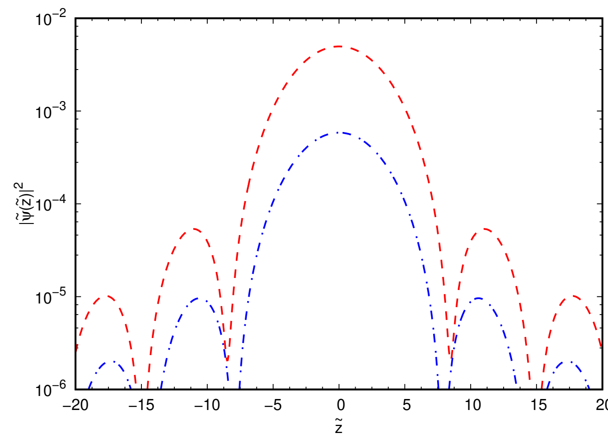

FIG. 9. Integrated probability density for the two spin components as a function of the rescaled longitudinal momentum. Dashed line: $\tilde{\psi}_{\uparrow\downarrow}(\tilde{z}) = \int_0^\infty db\tilde{\psi}_{\uparrow\downarrow}(\tilde{z}, b)$ and dash-dotted line: $\tilde{\psi}_{\uparrow\uparrow}(\tilde{z}) = \int_0^\infty db\tilde{\psi}_{\uparrow\uparrow}(\tilde{z}, b)$.

Light-front holographic wf

G. A. Miller and S. J. Brodsky, arXiv:1912.08911 [hep-ph]

Summary

- QCD inspired fermionic BSE model
- Solution in Minkowski space via Nakanishi Int. Representation;
- pion: LF amplitudes, SL FF, Valence: GPD, TMD,PDF
- Image of the pion (Ioffe-time & impact parameter)

Future ...

- Self-energies, Landau gauge, quark-gluon vertex: ingredients from LQCD
- Confinement & quark-gluon vertex?
- Beyond the pion, kaon, D, B, rho…, and the nucleon
- TL FF, GPDs (DGLAP&ERBL),
- GTMDs (DGLAP&ERBL),
- Fragmentation Functions...

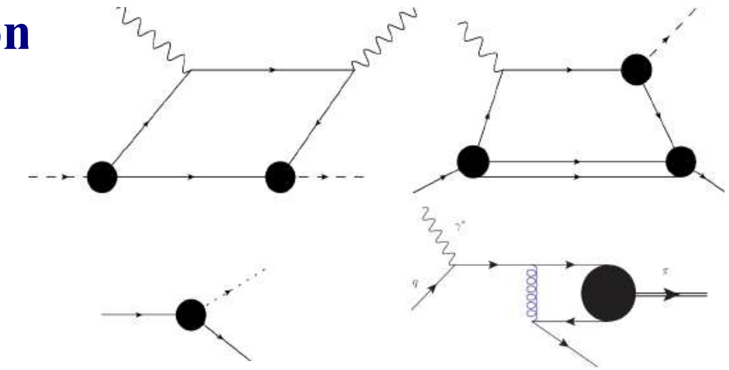

THANK YOU!

Observables associated with the hadron structure

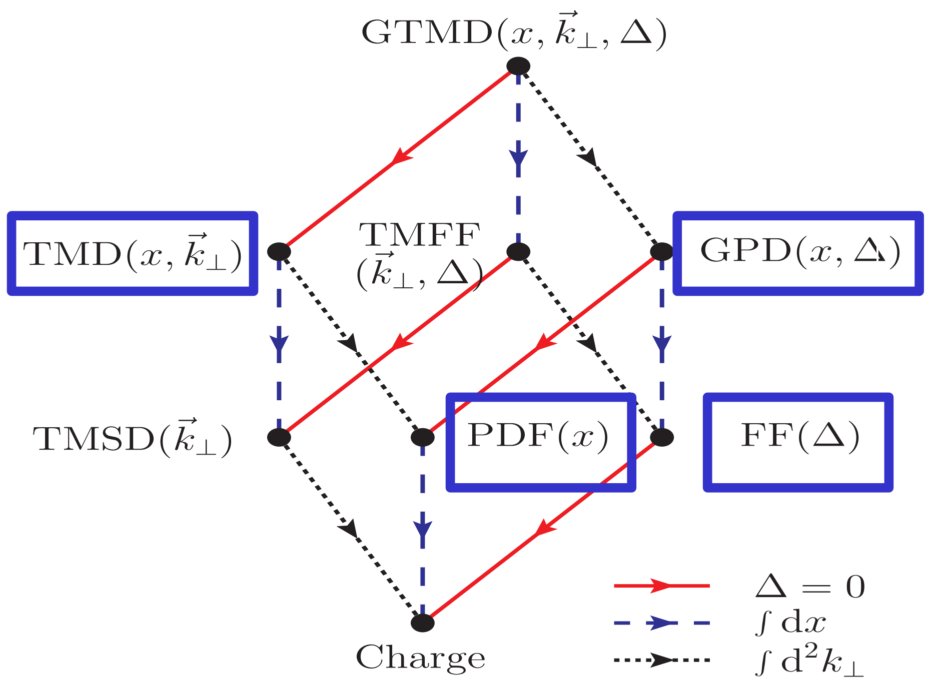

Lorcé, Pasquini, Vanderhaeghen JHEP05(2011)041

- TMD, PDFs, SL and TL form factors (pion) …

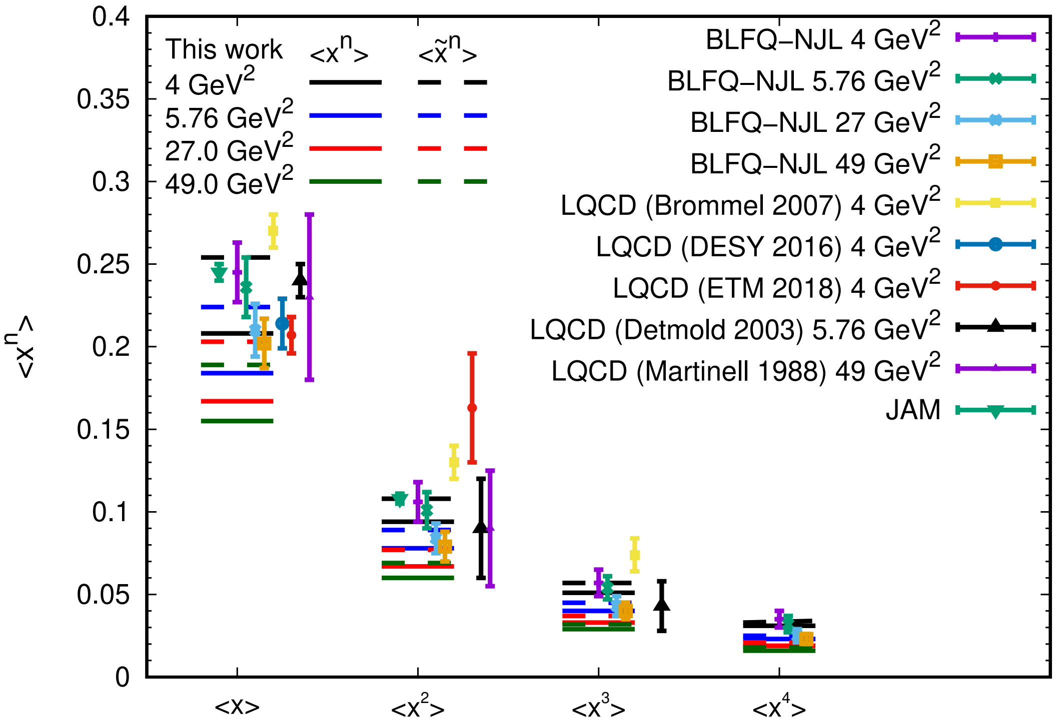

FIG. 6. Moments of the pion parton distribution for the parameter set VII at several scales Q^2 compared to different models, Lattice and the JAM global fit at 4 GeV^2[36]. Results are shown both for the original $\phi(\xi)$ (solid lines) and using the phenomenological treatment given by Eq. (49) (dashed lines). The results are compared with BLFQ NJL calculations of [39, 40]. The lattice results are from Brommel et al [41], DESY [42], ETM [37], Detmold [43] and Martinell [44].

Schematic view: TMDs & PDFs

FSI gluon exchange: T-odd

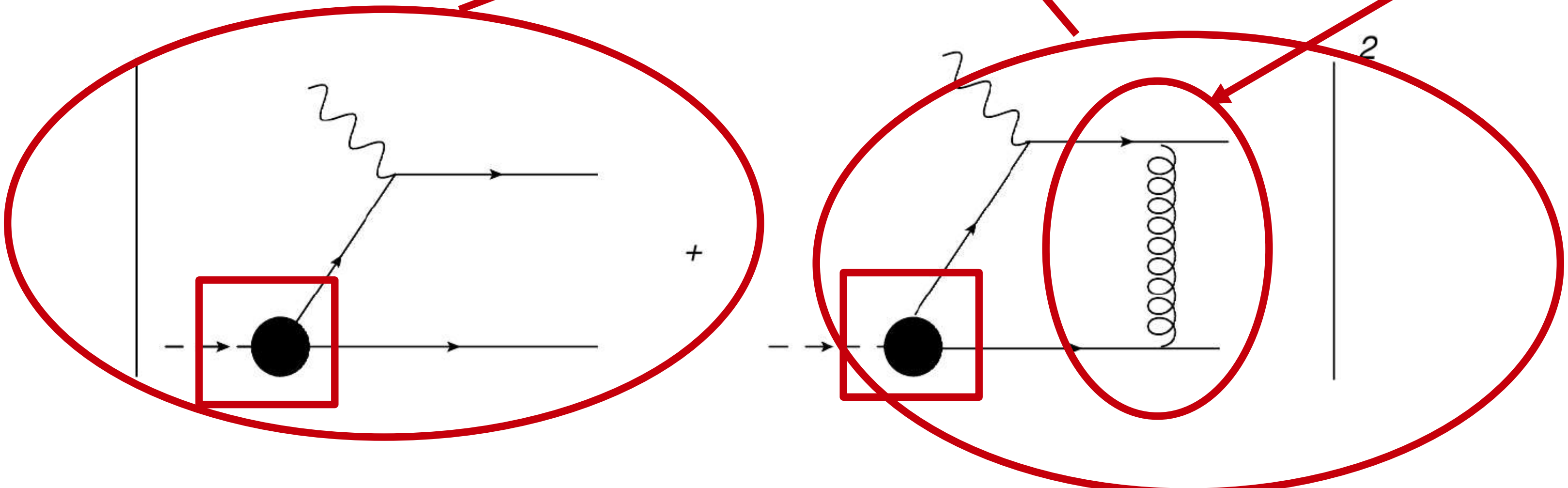

TF & Miller PRD 50 (1994)210

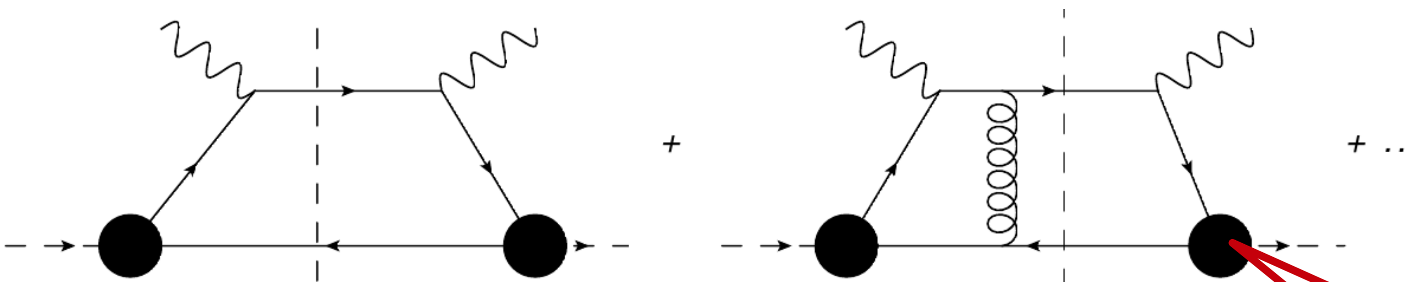

$$q^2 = q^+q^- - q^2_T$$

$$q^+ = q^0+q^3 \quad q^- = q^0-q^3$$

$q^- \longrightarrow$ *infty*
DIS

Bethe-Salpeter Amplitude @ x^+=0

Bethe-Salpeter amplitude: beyond the valence states

Light-front projection

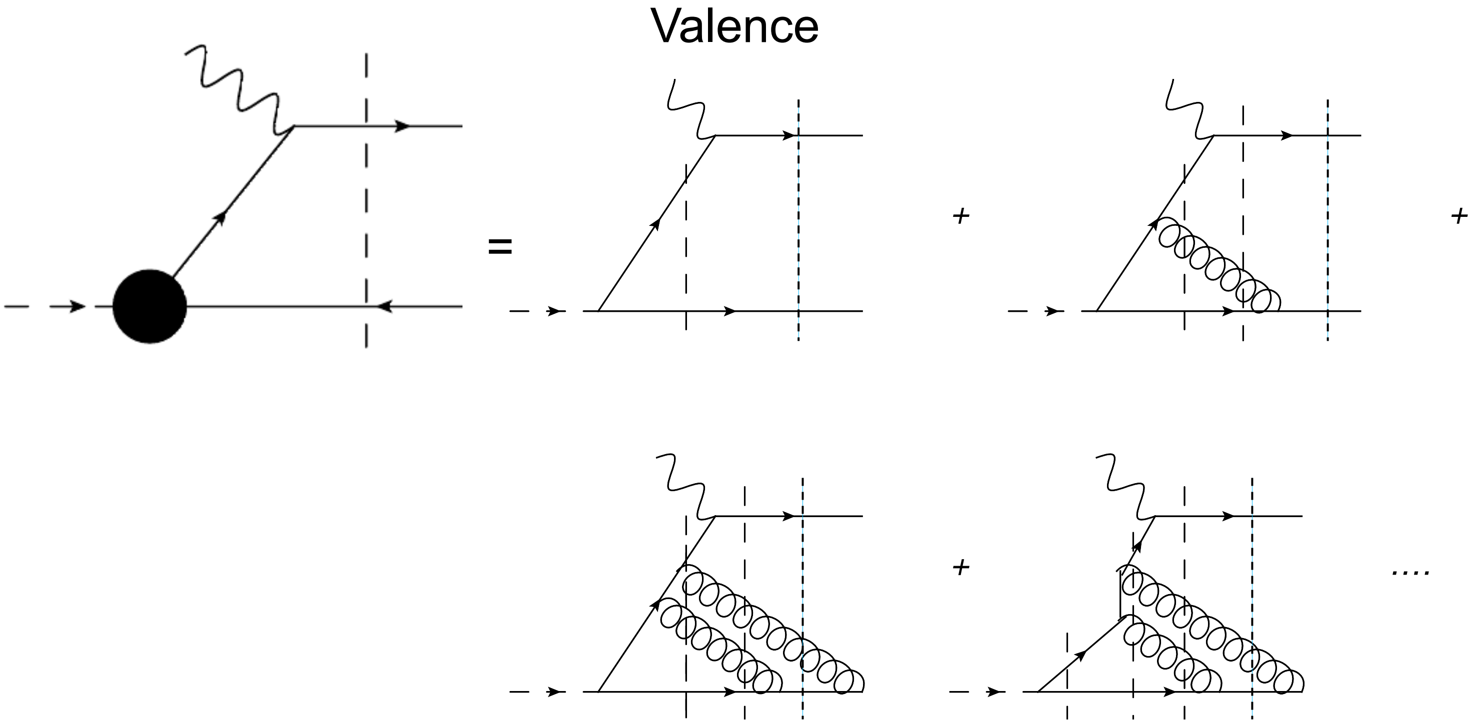

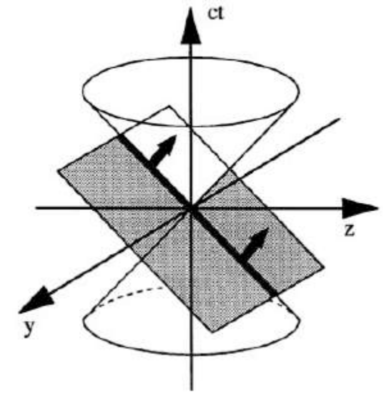

- **higher Fock-components**
- **gluon radiation = initial state interaction (ISI)**
- **gluon radiation in the final state (FSI)**

Sales, TF, Carlson,Sauer, PRC 63, 064003 (2001); Marinho, TF, Pace,Salme,Sauer, PRD 77, 116010 (2008)

Generalized Stietjes transform and the LF valence wave function II

Carbonell, TF, Karmanov PLB769 (2017) 418

$$f(\gamma) \equiv \int_0^\infty d\gamma' \, L(\gamma, \gamma') g(\gamma') = \int_0^\infty d\gamma' \, \frac{g(\gamma')}{(\gamma' + \gamma + b)^2}$$

denoted symbolically as $f = \hat{L}\, g$.

$$g(\gamma) = \hat{L}^{-1} f = \frac{\gamma}{2\pi} \int_{-\pi}^{\pi} d\phi \; e^{i\phi} \; f(\gamma\, e^{i\phi} - b).$$

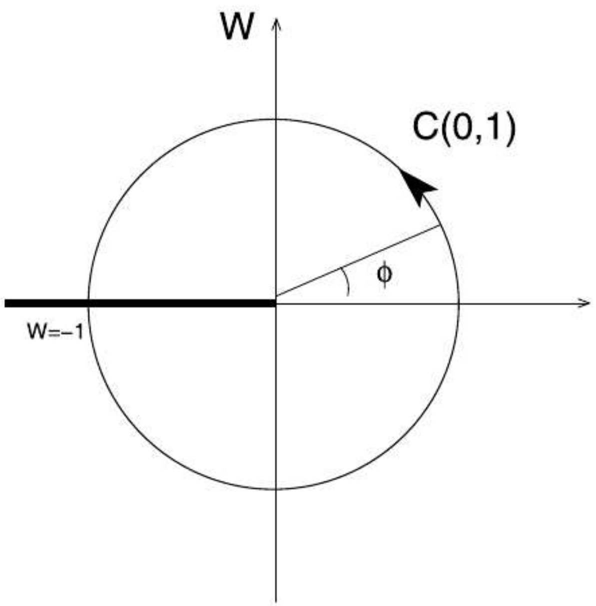

J.H. Schwarz, J. Math. Phys. 46 (2005) 014501,

- Kernel of the LF projected pion BSE with NIR
- end-point singularities in the k⁻ integration (zero-modes)

T.M. Yan , Phys. Rev. **D 7**, 1780 (1973)

$$\mathcal{I}(\beta, y) = \int_{-\infty}^{\infty} \frac{dx}{\left[\beta x - y \mp i\epsilon\right]^2} = \pm \frac{2\pi i \; \delta(\beta)}{\left[-y \mp i\epsilon\right]}$$

→ Kernel with delta and its derivative!

End-point singularities– more intuitive: can be treated by the pole-dislocation method
de Melo et al. NPA631 (1998) 574C, PLB708 (2012) 87